Available online at www.sciencedirect.com
ScienceDirect

Earth and Planetary Science Letters 256 (2007) 577–587

EPSL

www.elsevier.com/locate/epsl

# Isotopic evidence for iron mobilization during Paleoproterozoic lateritization of the Hekpoort paleosol profile from Gaborone, Botswana

Kosei E. Yamaguchi [a,b,c,*], Clark M. Johnson [b,c], Brian L. Beard [b,c], Nicolas J. Beukes [c,d], Jens Gutzmer [d], Hiroshi Ohmoto [c,e]

[a] *Institute for Research on Earth Evolution (IFREE), Japan Agency for Marine-Earth Science and Technology (JAMSTEC), 2-15 Natsushima, Yokosuka, Kanagawa 237-0061, Japan*
[b] *Department of Geology and Geophysics, University of Wisconsin, Madison, 1215 W. Dayton St., Madison, WI 53706, USA*
[c] *NASA Astrobiology Institute, USA*
[d] *Department of Geology, University of Johannesburg, P.O. Box 524, Auckland Park 2006, Johannesburg, South Africa*
[e] *Astrobiology Research Center and Department of Geosciences, The Pennsylvania State University, University Park, PA 16802, USA*

Received 13 July 2006; received in revised form 29 January 2007; accepted 5 February 2007
Available online 13 February 2007
Editor: R.W. Carlson

---

## Abstract

The isotopic composition and elemental abundance of Fe in a lateritic weathering profile (drillcore Strata-1) formed on the ~2.2 Ga Hekpoort basalt of the Pretoria Group in Gaborone, Botswana, document open-system behavior for Fe during paleosol formation. The $\delta^{56}$Fe values of the profile increase from ~0‰ at the bottom (parental basalt) to +1‰ in the mid-depth mottled (Fe-depleted) zone, then decrease to +0.3‰ at the top of the laterite (Fe-enriched) zone. The reworked ferricrete and red beds that overlie the laterite have high $\delta^{56}$Fe values of +0.2 to +0.4‰, which are comparable to those of the underlying laterite. Because of the absence of a complementary low-$\delta^{56}$Fe zone, these results are not compatible with a model of simple internal redistribution (closed-system) of Fe within the paleosol column. Instead, these results are well explained through fluid–rock interaction involving transport of aqueous $Fe^{2+}$ through the system during paleosol evolution. Production of positive $\delta^{56}$Fe values for $Fe^{3+}$ oxides were simulated through oxidation of low-$\delta^{56}$Fe $Fe^{2+}_{aq}$ using experimentally determined $Fe^{3+}_{oxide}$–$Fe^{2+}_{aq}$ fractionation factors. The increased quantities of $Fe^{2+}$ involved in formation of the Hekpoort paleosol relative to previous estimates based on a closed-system model require a commensurate increase in the abundance of an oxidant, such as atmospheric $O_2$, to explain the $Fe^{3+}/Fe^{2+}$ ratios in the paleosol. Therefore, previous estimates of atmospheric $O_2$ levels of $2.5\times10^{-4}$ to $9\times10^{-3}$ atm based on this section [W. Yang, H.D. Holland, The Hekpoort paleosol profile in Strata 1 at Gaborone, Botswana: Soil formation during the great oxidation event, American Journal of Science 303(2003) 187–220] are too low by an order of magnitude or more. These results demonstrate that Fe isotopes can provide important constraints on open- *versus* closed-system behavior of Fe in ancient weathering profiles, a distinction that is critical when calculating Fe mobility as a means for inferring surface redox conditions in the past.

*Keywords:* paleosol; Fe; isotope; weathering

---

[*] Corresponding author. Institute for Research on Earth Evolution (IFREE), Japan Agency for Marine-Earth Science and Technology (JAMSTEC), 2-15 Natsushima, Yokosuka, Kanagawa 237-0061, Japan.
*E-mail address:* kosei@jamstec.go.jp (K.E. Yamaguchi).

0012-821X/$ - see front matter © 2007 Elsevier B.V. All rights reserved.
doi:10.1016/j.epsl.2007.02.010

## 1. Introduction

The relative mobility of Fe in Paleoproterozoic paleosols has been used to constrain the timing of proposed increases in atmospheric $O_2$ contents, where net Fe losses are interpreted to reflect Fe mobilization during weathering under an anoxic atmosphere, and Fe retention is interpreted to reflect oxidation "in place" during weathering under an $O_2$-bearing atmosphere (*e.g.*, [2]). Iron distributions in paleosols (*e.g.*, [2–5]), as well as other geochemical data (*e.g.*, [6]), have been used to infer a rapid increase in the partial pressure of atmospheric $O_2$ ($pO_2$) at ~2.3 Ga, which has been termed the Great Oxidation Event (GOE; [7,8]). In contrast, some workers have challenged the idea of the Paleoproterozoic GOE, instead suggesting that Earth's atmosphere had relatively high $pO_2$ levels since the Archean (*e.g.*, [9,10]).

The 2.2 Ga paleosols that developed on the Hekpoort lavas of the Pretoria Group (Fig. 1) at Waterval Onder in the eastern Transvaal and those in the central Transvaal near Pretoria, South Africa, are particularly important because they have been considered to be one of the youngest Fe-depleted paleosols [2,11], potentially placing constraints on the $pO_2$ level and the timing of the GOE (*e.g.*, [2]). Rye and Holland [11] initially estimated a $pO_2$ level of $\leq 8 \times 10^{-4}$ atm, based on the major- and trace-element geochemistry of several sequences of the Hekpoort paleosol and assumptions of losses of Fe from the paleosol sections. Beukes et al. [12], however, noted that these sections represented only the lower part of lateritic weathering profiles where the upper parts were eroded during and/or before deposition of overlying sediments. They documented a complete laterite section at Gaborone in Botswana (Figs. 1 and 2). Based on study of the complete section at Gaborone, Yang and Holland [1] revised their estimate of $pO_2$ levels at 2.2 Ga to $2.5 \times 10^{-4}$ to $9 \times 10^{-3}$ atm, a factor of 23 to 840 less than the present day, recognizing that some oxidation of Fe occurred during paleosol formation.

A critical aspect of Yang and Holland's calculations lies in their interpretation that only internal redistribution of Fe occurred within the paleosol section, where they argued that no net transport of Fe occurred in or out of the section. Demonstration of no net Fe loss or addition is critical to estimation of the moles of Fe that may have been oxidized by atmospheric $O_2$, and this is key to the $pO_2$ levels calculated by Yang and Holland [1]. In contrast, Beukes et al. [12] suggested that the Hekpoort laterite profiles were developed through processes that were similar to those that occur in modern laterites, where $Fe^{3+}$ and $Fe^{2+}$ are leached from rocks by downward moving soil water and laterally flowing groundwater, aqueous $Fe^{2+}$ is oxidized to $Fe^{3+}$-(hydr)oxides by molecular $O_2$, and $Fe^{3+}$-(hydr)oxides-rich zones migrate deeper with evolution of the soil

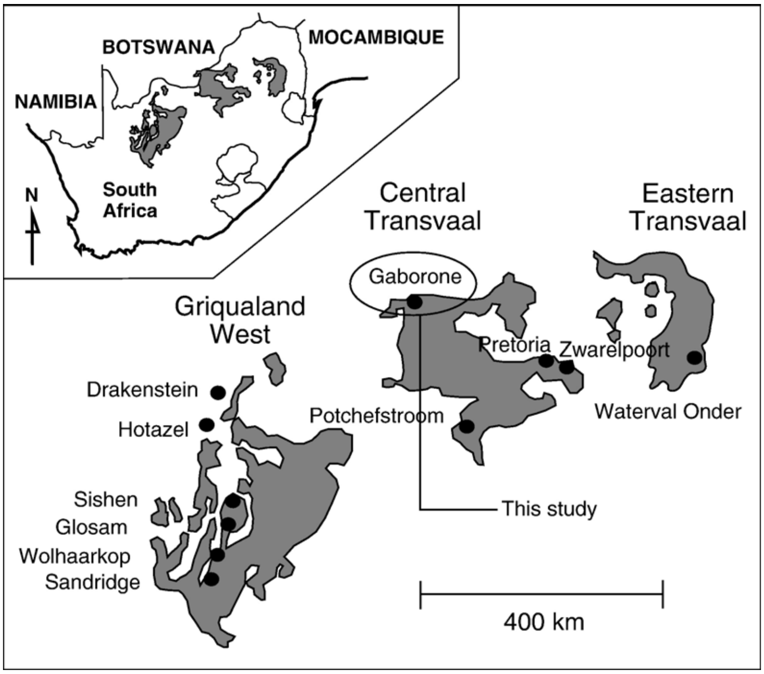

Fig. 1. Occurrences of ~2.2 Ga lateritic paleosols (solid circles) in southern Africa. Data from Evans et al. [18].

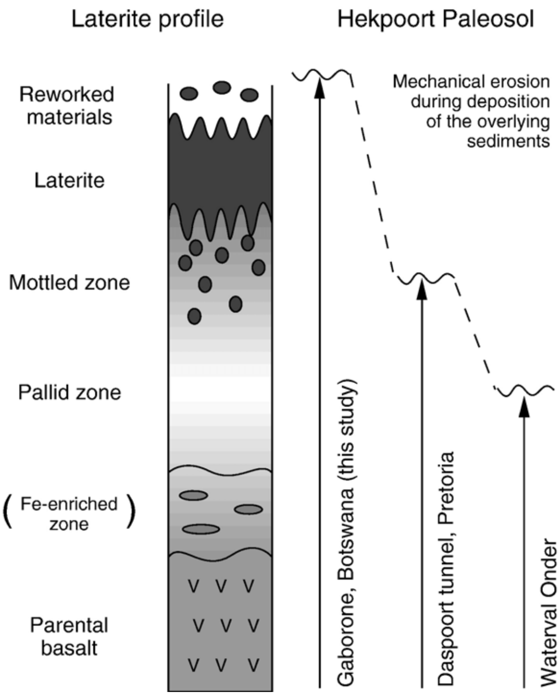

Fig. 2. Diagram illustrating modern laterite weathering profile (left) and the inferred correlative sections of the Hekpoort paleosol that are exposed at Gaborone, Daspoort tunnel, and Waterval Onder.

profile. Their model postulates open-system transport of Fe, where Fe was mobilized by organic acids.

In this study, we investigate Fe isotope variations in the complete section of the Hekpoort paleosol studied by Beukes et al. [12] and Yang and Holland [1]. Isotopic mass–balance constraints provide a sensitive means for evaluating the extent of Fe mobilization and open- or closed-system behavior. In addition, the sensitivity of Fe isotope fractionation factors to redox state (*e.g.*, [13]) may constrain the mechanisms and oxidation state of Fe mobilization in paleosols, which ultimately may place constraints on ancient atmospheric $O_2$ levels.

## 2. Geology of the Hekpoort paleosols

The Hekpoort paleosol is a regional paleoweathering horizon that was developed on the ~2.25 Ga Hekpoort basaltic lavas [14] of the Pretoria Group, Transvaal Supergroup. The Hekpoort Basalt have been only weakly metamorphosed to lower greenschist facies [15,16]. The paleosol is overlain by an erosional contact with the Dwaalheuvel Formation of the Pretoria Group. Based on paleomagnetic data, Evans et al. [17,18] suggested that the laterites formed in an equatorial setting. Paleosol formation occurred between 2.22 and 2.06 Ga [12,15,19,20].

The Hekpoort paleosol at the Waterval Onder locality has been frequently described in the literature, and is generally considered to consist of, in ascending order, fresh basaltic lava, partly altered lava (saprolite), and an Fe-depleted pallid zone [1,11,12]. The pallid zone had been interpreted by earlier investigators [4,5] to represent the top of the paleosol profile. This was the reason that Holland [4,7] considered the Hekpoort paleosol as the best example of an Fe-depleted paleosol. Beukes et al. [12], however, discovered an Fe-rich upper portion of the paleosol based on drillcores from near Gaborone in Botswana and Potchefstroom in the western Transvaal. These drillcores provide a complete section of the Hekpoort paleosol that is quite similar to modern laterite profiles. The Hekpoort paleosol in the central and eastern Transvaal are now recognized as partial sections where the upper laterite and mottled zones were eroded during and/or prior to deposition of the overlying Dwaalheuvel Formation [12]. In the western Transvaal, the Hekpoort laterite profile is overlain by a reworked laterite or ferricrete [21], which is composed of hematite-cemented and hematite-coated red and white clay clasts that were derived from the underlying lateritic regolith [12].

## 3. Samples and analytical methods

Fifteen samples were taken from the drillcore Strata-1 recovered near Gaborone, Botswana (Figs. 1 and 2). This drillcore has been previously studied by Beukes et al. [12] and Yang and Holland [1], and these studies report chemical analyses for the section. The samples analyzed for Fe isotope compositions include one fresh Hekpoort Basalt at the bottom, seven samples from the mid-depth pallid and mottled zones, one sample from the top of the lateritic paleosol, two samples from the overlying reworked laterite, and four samples from the overlying red beds of the Dwaalheuvel Formation.

Powdered samples were completely digested in heated Teflon beakers using concentrated HF and $HNO_3$. Iron was separated from the bulk sample using anion-exchange chromatography and anion exchange resin (Bio-Rad AG 1X4 200–400 mesh). Iron contents of the separated solution were determined using the *Ferrozine* method [22], which allowed Fe concentrations for MC–ICP–MS analysis to be matched to those of standards and to check that ion-exchange column yields were 100%. Iron isotope analyses were made by MC–ICP–MS (Micromass *IsoProbe*) equipped with a collision cell and a micro-concentric desolvating nebulizer (Cetac *Aridus*) at the University of Wisconsin — Madison. A mixture of pure hydrogen and argon gases was used in the collision cell of the *IsoProbe* in order to remove all ArO and ArN interferences on the Fe mass spectrum, as well as essentially all ArOH species. A standard-sample-standard bracketing method was used to correct for instrumental mass bias, which produces accurate results if the separated Fe solutions are pure, such that the sample matrix matches that of the standards [23]. Obtaining pure Fe separations during chemical processing is essential for not only eliminating isobars but also eliminating matrix effects that change the mass bias for a particular sample relative to that of adjacent standards [24].

Iron isotope compositions are reported in Table 1 using standard delta ($\delta$) notation in per mil (‰) relative to the average of igneous rocks [24]: $\delta^{56}Fe=[(^{56}Fe/^{54}Fe)_{sample}/(^{56}Fe/^{54}Fe)_{igneous\ rocks}-1]\times10^3$. Comparison between laboratories may be made through the IRMM-14 Fe standard, which has a $\delta^{56}$Fe value of $-0.09\pm0.05$‰ [24] on the igneous rock scale. Reproducibility in $\delta^{56}$Fe values is ±0.05‰ based on the precision of three standards that were run during the time period in which samples were measured: UW J–M Fe: $\delta^{56}Fe=+0.25\pm0.05$‰ ($n=47$), $\delta^{57}Fe=+0.39\pm0.07$‰; UW HPS Fe: $\delta^{56}Fe=+0.49\pm0.05$‰, $\delta^{57}Fe=+0.74\pm0.07$‰ ($n=52$); IRMM-14 Fe: $\delta^{56}Fe=-0.09\pm0.05$‰, $\delta^{57}Fe=-0.11\pm0.07$‰ ($n=54$), where all uncertainties are $1\sigma$ external standard deviations. Further details on analytical methods may be found in [24,25].

## 4. Results

Total Fe contents (expressed as wt.% $Fe_2O_3$) vary greatly in the paleosol relative to those of fresh Hekpoort basalt (9.4 wt.%), including very low (~0 wt.%) and very high (>50 wt.%) contents (Fig. 3). Previous work on the same drillcore provides a context for the current study. Fresh Hekpoort Basalt has homogenous $TiO_2$ contents ($0.66\pm0.05$ wt.%; $n=11$), and these increase in the sericite zone ($1.45\pm0.16$ wt.%; $n=11$) and mottled zone ($1.55\pm0.34$ wt.%; $n=7$) by more than a factor of two (Fig. 3). The molar Al/Ti ratios are relatively constant ($36.8\pm3.7$; $n=50$) throughout the lateritic paleosol profile (excluding the ferricrete section), contrasting with the highly variable $Fe^{3+}/Ti$ ($4.6\pm5.1$) and $Fe^{2+}/Ti$ ($10.3\pm9.0$) ratios (see Fig. 3; [1,12]). The $Fe^{3+}/\Sigma Fe$ (ferric Fe to total Fe) ratios are significantly higher in the upper paleosol sections (mottled/sericite zone: $0.61\pm0.26$; $n=18$) and the overlying ferricrete zone ($0.83\pm0.14$; $n=3$) and red beds ($0.66\pm0.21$; $n=13$), as compared to fresh Hekpoort basalt ($0.27\pm0.02$; $n=11$) and the overlying pallid zone ($0.25\pm0.07$; $n=24$) (Fig. 3; [1,12]). Most samples analyzed for Fe isotope compositions were taken from the paleosol sections (102 to 130 m depth) that vary greatest in $Fe^{3+}/Ti$ and $Fe^{2+}/Ti$ ratios, and $\delta^{56}$Fe values are highly variable (−0.1–+1.0‰) in these sections (Fig. 3).

An important observation is that for all samples but one, the $\delta^{56}$Fe values of the paleosol are positive throughout the profile, where the average is $+0.39\pm0.33$ ($1\sigma$)‰ ($n=15$). This contrasts with the restricted range in $\delta^{56}$Fe values for most igneous rocks, which have $\delta^{56}Fe=0.00\pm0.05$; some high-$SiO_2$ granites have slightly higher $\delta^{56}$Fe values [24–26]. The $\delta^{56}$Fe value for the fresh Hekpoort basalt sample is identical to the average of igneous rocks within error. The $\delta^{56}$Fe values of the lateritic Hekpoort paleosol are also significantly

Table 1
Data for the Paleoproterozoic lateritic Hekpoort paleosol from Gaborone, Botswana

| Sample ID | Depth (m) | Individual analyses | | | | $\Sigma Fe_2O_3$ (wt.%) | Lithology |
|---|---|---|---|---|---|---|---|
| | | $\delta^{56}$Fe (‰) | 2-SE (‰) | $\delta^{57}$Fe (‰) | 2-SE (‰) | | |
| BTW-01 | 90.30 | 0.14 | 0.06 | 0.19 | 0.03 | 7.8 | Ferricrete/red beds |
| BTW-02 | 91.90 | 0.09 | 0.05 | 0.14 | 0.03 | 31.5 | Ferricrete/red beds |
| BTW-03 | 99.80 | 0.23 | 0.04 | 0.36 | 0.03 | 7.9 | Ferricrete/red beds |
| BTW-04 | 101.27 | 0.52 | 0.08 | 0.68 | 0.03 | 17.4 | Ferricrete/red beds |
| BTW-05 | 102.50 | 0.18 | 0.07 | 0.26 | 0.04 | 39.4 | Laterite |
| BTW-06 | 102.60 | 0.43 | 0.07 | 0.66 | 0.03 | 48.9 | Laterite |
| BTW-07 | 103.00 | 0.34 | 0.08 | 0.47 | 0.04 | 29.4 | Mottled zone |
| BTW-08 | 103.20 | 0.47 | 0.05 | 0.67 | 0.03 | 2.7 | Mottled zone |
| BTW-09 | 104.53 | 0.53 | 0.05 | 0.69 | 0.03 | 21.3 | Mottled zone |
| BTW-10 | 104.56 | 0.57 | 0.06 | 0.82 | 0.03 | 19.0 | Mottled zone |
| BTW-11 | 104.60 | 1.04 | 0.05 | 1.52 | 0.03 | 0.004 | Mottled zone |
| BTW-12 | 105.26 | 1.04 | 0.06 | 1.58 | 0.03 | 0.08 | Pallid zone |
| BTW-13 | 106.10 | 0.31 | 0.05 | 0.49 | 0.03 | 1.4 | Pallid zone |
| BTW-14 | 107.33 | −0.12 | 0.03 | −0.15 | 0.02 | 6.1 | Pallid zone |
| BTW-15 | 128.12 | 0.05 | 0.04 | 0.09 | 0.03 | 9.4 | Parental rock |

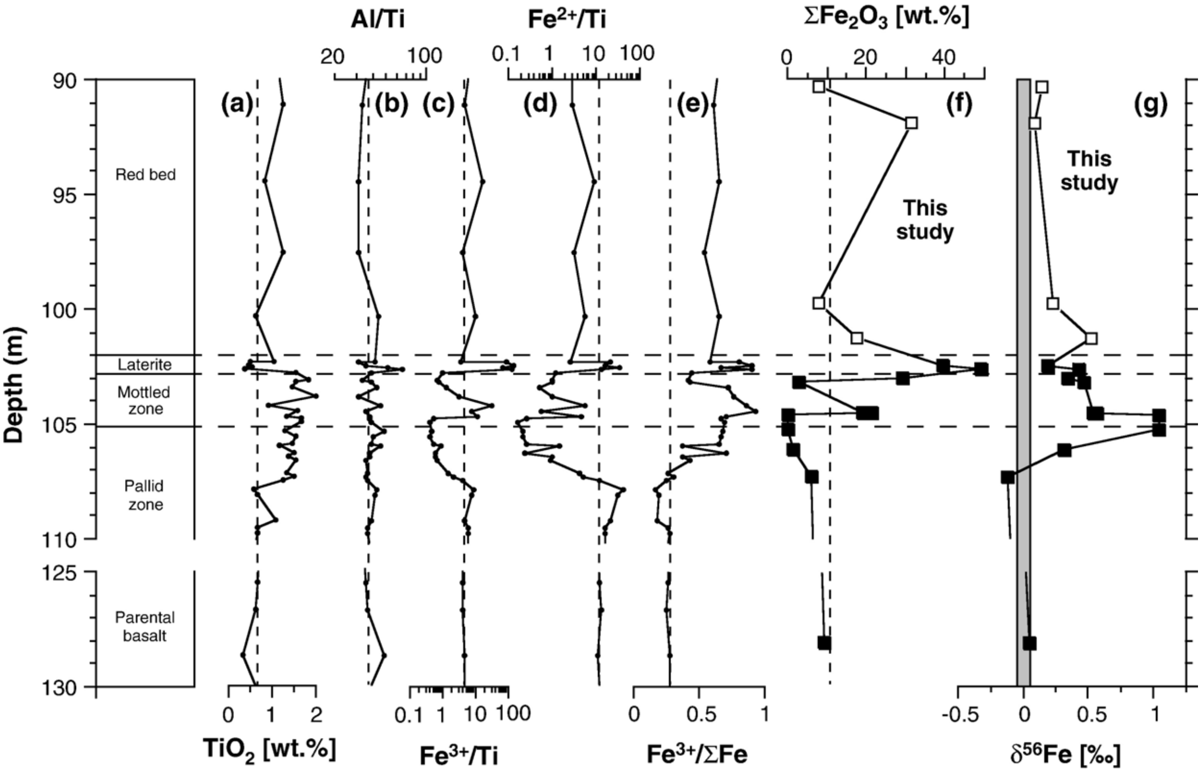

Fig. 3. Depth profile of (a) $TiO_2$ contents, (b) molar Al/Ti ratios, (c) molar $Fe^{3+}$/Ti ratios, (d) molar $Fe^{2+}$/Ti ratios, (e) $Fe^{3+}/\Sigma Fe$ ratios, (f) total Fe contents (as wt.% $\Sigma Fe_2O_3$), and (g) Fe isotope compositions for the lateritic profile of the Hekpoort paleosol in drillcore Strata-1 from near Gaborone, Botswana. Data for (a) through (e) are taken from Yang and Holland [1]. In (f) and (g), filled symbols represent lateritic weathering profile and open symbols represent reworked materials. Dashed lines in (a) through (f) represent average values of parental basalt section calculated from Yang and Holland [1]. In (g), gray bar at $\delta^{56}Fe = 0.00 \pm 0.05$‰ indicates the average for igneous rocks [24], which is similar to the average of low-$C_{org}$, -$C_{carb}$ clastic rocks [27,28].

higher than the average of low-$C_{org}$ (organic carbon) or low-$C_{carb}$ (carbonate carbon) clastic sedimentary rocks, which scatter closely about $\delta^{56}Fe = 0$‰, as well as high-$C_{org}$ clastic sedimentary rocks, which are skewed toward negative $\delta^{56}$Fe values (typically ∼−2‰) [27,28].

In general, the $\delta^{56}$Fe values increase upward in the section (Fig. 3) from the parental basalt ($\delta^{56}Fe = +0.05$‰), through the Fe-depleted pallid zone, to the mottled zone, where $\delta^{56}$Fe values peak at +1.04‰, and the average $\delta^{56}$Fe value for the mottled and pallid zones is +0.52±0.38‰ ($n=8$). The $\delta^{56}$Fe values decrease upward within the mottled zone to the top of the laterite profile ($\delta^{56}Fe = +0.18$‰) (Fig. 3). The overlying reworked ferricrete and red beds have moderately positive $\delta^{56}$Fe values ranging from +0.09 to +0.52 (average $\delta^{56}Fe = +0.25 \pm 0.19$‰; $n=4$). These high $\delta^{56}$Fe values are similar to those of the underlying laterite.

Fig. 4 shows the relations between $\delta^{56}$Fe and total Fe contents (expressed as wt.% $Fe_2O_3$) of the laterite profile. Both the Fe-depleted and Fe-enriched zones have higher $\delta^{56}$Fe values relative to fresh Hekpoort basalt (Fig. 4). For the samples that have total Fe contents less than those of the parental basalt, the $\delta^{56}$Fe values tend to increase with decreasing Fe contents (Fig. 4), and this is found in samples from the laterite profile, as well as samples from the overlying reworked zone. The $\delta^{56}$Fe values for all Fe-enriched samples are positive, but are not correlated with total Fe contents (Fig. 4).

## 5. Discussion

Iron isotope data for the Hekpoort paleosol help resolve the conflicting models that have been proposed for its origin [1,12] by providing constraints on open- or closed-system behavior of Fe. Twenty-four of the twenty-five Hekpoort paleosol samples have positive $\delta^{56}$Fe values that are higher than the $\delta^{56}$Fe value of the parental basalt (*i.e.*, ∼0‰), which requires that the

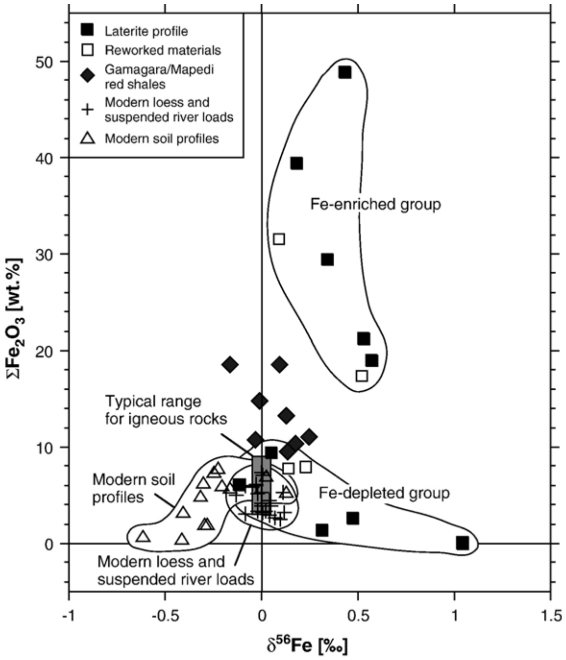

Fig. 4. Cross plot of total Fe contents (as wt.% $\Sigma Fe_2O_3$) *versus* Fe isotope compositions for the lateritic paleoweathering profile of the Hekpoort paleosol in drillcore Strata-1 from near Gaborone, Botswana. Samples are divided into an "Fe-enriched group" (three samples from laterite profile and four samples from reworked materials) and an "Fe-depleted group" (six samples from laterite profile and two samples from reworked materials). Also shown are red shales of the 2.2 Ga Gamagara/Mapedi Formation in South Africa (filled diamonds; [28,29]), modern suspended river loads and modern loess (crosses; [27]), and modern soil profiles (open triangles; [31,34]). All Fe isotope data calculated in terms of $^{56}Fe/^{54}Fe$ ratios on the igneous rock scale [24]. Shaded rectangle indicates a typical range for igneous rocks ($\Sigma Fe_2O_3 = 3–9$ wt.% and $\delta^{56}Fe = 0.00 \pm 0.05$‰).

Hekpoort paleosol developed as an open system with respect to Fe. These constraints in turn affect the validity of calculated $pO_2$ levels, which are dependent upon understanding the molar Fe budget of the paleosol.

### 5.1. Comparison with other weathering products

The systematic changes in major-element compositions upsection from the Hekpoort basalt, where molar Ca/Ti, Na/Ti, Mg/Ti, and Mn/Ti ratios decrease, $TiO_2$ contents increase, but molar Al/Ti ratios remain constant (Fig. 3; [1,12]), strongly support the interpretation that the section represents a paleosol; such stratigraphically-related chemical variations cannot be explained through hydrothermal alteration or by the effects of regional greenschist-facies metamorphism [12]. The red beds of the overlying Dwaalheuval and Gamagara/Mapedi Formations are also depleted in Na, Ca, Mg, and variably enriched in Fe [12,28,29], yet their $\delta^{56}Fe$ values are relatively restricted as compared to the Hekpoort paleosol (Figs. 3 and 4). For example, although the ~2.2 Ga red beds in the Gamagara/Mapedi Formation are enriched in Fe relative to igneous rocks and have high $Fe^{3+}/\Sigma Fe$ ratios ($0.83 \pm 0.16$; $n = 11$), their $\delta^{56}Fe$ values ($+0.08 \pm 0.12$‰; $n = 11$) [28] scatter about the average for igneous rocks (0‰) and overlap those of modern suspended river loads and loess that likely reflect the average of continental crust (Fig. 4; [27]). These observations indicate that some surface weathering products show little change in $\delta^{56}Fe$ values for bulk material despite significant changes in $Fe^{3+}/\Sigma$ Fe ratios, suggesting that such material "rusted in place" and that Fe behaved as a conservative element. The lack of significant Fe loss, as required by the restricted range in Fe isotope compositions, is expected during weathering under an $O_2$-bearing atmosphere [30].

In contrast, mobilization of Fe in modern soils may be accompanied by Fe isotope fractionation if Fe is mobilized by organic acids or oxides are partially reduced by bacterial $Fe^{3+}$ reduction. Fantle and DePaolo [31] report Fe isotope data for bulk samples from a modern soil profile, where $\delta^{56}Fe$ values vary from −0.6 to +0.1‰, and the lowest $\delta^{56}Fe$ values occur in the samples that contain the lowest Fe contents (Fig. 4) at the top of profile. This trend suggests preferential loss of a high-$\delta^{56}Fe$ component occurred from the upper soil horizon. Fantle and DePaolo [31] also report Fe isotope data for acid (0.5 M HCl) leaches for the same sample set. A trend of increasing $\delta^{56}Fe$ values with decreasing acid-leached Fe contents indicates the presence of a significant low-$\delta^{56}Fe$ component in the soil profile, which they speculate may be organically bound $Fe^{3+}$. The tendency for soluble, organically-bound $Fe^{3+}$ to have low-$\delta^{56}Fe$ values has been demonstrated in silicate-leaching experiments [32,33].

Emmanuel et al. [34] compared the Fe isotope distribution in forest and semi-arid soil profiles, and bulk soil samples had $\delta^{56}Fe$ values between −0.1 and −0.5‰. As in the soil profile studied by Fantle and DePaolo [31], Emmanuel et al. [34] found that the lowest $\delta^{56}Fe$ values for bulk soil tend to occur in samples that have the lowest Fe contents. Through mixing relations between the quantities of Fe bound in silicate-, oxide-, and organic-extractable components, they inferred that the organically-bound $Fe^{3+}$ had $\delta^{56}Fe$ values of approximately −0.4‰, whereas the $Fe^{3+}$ oxide component had more fractionated isotopic compositions of $\delta^{56}Fe = -0.8$ to −1.2‰. The silicate-bound component was inferred to have a $\delta^{56}Fe$ value near zero within uncertainty, identical to the average of igneous rocks or low-$C_{org}$,-$C_{oarb}$ clastic rocks [24,27]. Emmanuel et al. [34] interpret the negative $\delta^{56}$Fe organic and oxide components to reflect the effects of organic binding (*e.g.*, [32,33]) and oxidation of Fe following reductive dissolution of oxides by $Fe^{3+}$-reducing bacteria, respectively.

It is important to note that low-$\delta^{56}$Fe oxides are not expected based on Fe isotope fractionation factors determined by theory or experiment [30], but could be produced by near complete oxidation and precipitation of low-$\delta^{56}$Fe aqueous $Fe^{2+}$, such as might occur when $Fe^{2+}_{aq}$ encountered an $O_2$-rich horizon during groundwater flow (*e.g.*, [35]). In addition to modern soil profiles, low-$\delta^{56}$Fe oxides have been found in marine sediments, including those on modern continental shelves [36,37] and Phanerozoic oxide-bearing limestones [38]. In all of these cases, bacterially-mediated redox cycling has been invoked as the means for initially producing the low-$\delta^{56}$Fe components that are eventually sequestered as $Fe^{3+}$ oxides.

In contrast to the Fe isotope variations observed in modern paleosols, the Hekpoort paleosol has positive $\delta^{56}$Fe values for both low- and high-Fe content samples (Fig. 4). In addition, the range in Fe isotope compositions and Fe contents greatly exceeds that observed in bulk samples of modern soils. The positive $\delta^{56}$Fe values, particularly for oxide-rich samples, suggest an overall process of partial oxidation of $Fe^{2+}_{aq}$ followed by oxide precipitation [39,30]. A single oxidation process or "event" cannot, however, simultaneously explain the high $\delta^{56}$Fe values in low- and high-Fe content samples. The low-Fe, high-$\delta^{56}$Fe Hekpoort samples could reflect loss of low-$\delta^{56}$Fe $Fe^{2+}_{aq}$, whereas the high-Fe Hekpoort samples require net addition of a high-$\delta^{56}$Fe component. These processes will be explored below.

### *5.2. Models for laterite formation in the Hekpoort basalt*

Yang and Holland [1] consider the Hekpoort paleosol to have developed in a closed system based on an overall Fe retention factor ($\Phi$) of 0.96 for the section at Gaborone. Net oxidation of the paleosol during its formation was recognized in the contrasting $\Phi$ for FeO (0.77) and $Fe_2O_3$ (1.47), and estimation of the moles of atmospheric $O_2$ required to partially oxidize Fe in the paleosol is the basis for their estimates of $pO_2$, assuming a closed system with respect to net Fe transport. Within the paleosol, however, Fe retention factors are quite variable, commensurate with the variations in $Fe^{3+}$/Ti and $Fe^{2+}$/Ti ratios (Fig. 3). Table 2 summarizes the variations in $\Phi$ for each unit of the lateritic paleoweathering profile, using the unit subdivisions of Yang and Holland [1]. The laterite unit has an average $\Phi$ value of 4.0±3.6 ($n=4$), significantly higher and more variable as compared to that for the mottled zone (0.5±0.8; $n=7$) and the sericite zone (0.2±0.3; $n=11$). The chlorite zone, or the Fe-enriched zone between the pallid zone and the parental basalt, has an average $\Phi$ value of 1.3±0.5 ($n=23$). Considering the variable retention factors for each unit of the lateritic paleoweathering profile, we suggest that the overall $\Phi$ cannot be used as an indicator of closed-system behavior of Fe, and this conclusion is supported by the Fe isotope data.

We would expect the Fe isotope variations in the paleosol section to be very small (*i.e.*, ~0.0±0.1‰) in the Yang and Holland [1] model, which postulates soil formation to have occurred under relatively anoxic conditions and where $\Phi$ variations are solely due to internal redistribution of Fe. Closed-system redistribution of Fe within the paleosol could produce some samples with negative $\delta^{56}$Fe values and some with positive $\delta^{56}$Fe values, but the average $\delta^{56}$Fe value should lie near zero for the section. Only a single sample, however, has a near-zero $\delta^{56}$Fe value (−0.12‰), and the average $\delta^{56}$Fe value for the Hekpoort section is +0.55±0.30‰ ($n=9$) (from pallid zone to laterite; Table 1 and Fig. 3).

In contrast, Beukes et al. [12] interpret the paleosol section at Gaborone to reflect Fe mobilization in an open system where groundwater transport was important. Mobilization of Fe is envisioned to have occurred during wet seasons, where reduced, organic–acid bearing soil-water and groundwater reduced reactive $Fe^{3+}$ oxides, and

Table 2
Retention factor ($\Phi$) without volume correction (data from [12])

| Zone | Sample ID | Depth range (m) | Thickness (m) | Number of samples | $\Phi$ | 1$\sigma$ |
|---|---|---|---|---|---|---|
| Laterite | 99WY8b–99WY10a | 102.3–102.7 | 0.4 | 4 | 4.0 | 3.6 |
| Mottled zone | 99WY10b –99WY16 | 102.8–104.5 | 1.7 | 7 | 0.5 | 0.8 |
| Sericite zone | 99WY17a–99WY26 | 104.7–107.1 | 2.4 | 11 | 0.2 | 0.3 |
| Chlorite zone | 99WY27a–99WY49 | 107.3–117.7 | 10.4 | 23 | 1.3 | 0.5 |
| Parental basalt | 99WY50–99WY60 | 118.8–132.1 | 13.3 | 10 | 1.0 | 0.2 |

Retention factors in this table were calculated as the average $(Fe_2O_3/TiO_2)_{sample}/(Fe_2O_3/TiO_2)_{basalt}$ ratios for each unit.

where any dissolved $O_2$ would be consumed through reactions with organic matter (Fig. 5). Organic-acid bearing soilwater is inferred to have been derived from microbial biomass. Complete or near-complete reduction of reactive $Fe^{3+}$ oxides would produce $\delta^{56}$Fe values for $Fe^{2+}_{aq}$ that would be similar to those of the initial oxide, which would have $\delta^{56}$Fe values near zero. In contrast, partial reduction, if it occurred incongruently, would be expected to produce $Fe^{2+}_{aq}$ that had negative $\delta^{56}$Fe values, either through reduction by organic acids [40] or by dissimilatory $Fe^{3+}$-reducing bacteria [41,42]. In both cases, the residual oxides should have positive $\delta^{56}$Fe values, as required by isotopic mass balance. We therefore interpret the high-$\delta^{56}$Fe, low-Fe content samples to reflect the residual Fe pool that remained after Fe mobilization. In the model of Beukes et al., this is interpreted to reflect Fe transport during wet seasons.

The high-$\delta^{56}$Fe, iron-rich sections of the Hekpoort paleosol are interpreted to reflect deposition during dry seasons, where evaporitic process may have become important [12]. In this case, relatively anoxic groundwater is envisioned to have carried $Fe^{2+}_{aq}$ upward where it was oxidized and precipitated as $Fe^{3+}$- oxides and $Fe^{3+}$-hydroxides when $Fe^{2+}_{aq}$ encountered $O_2$ that diffused from the atmosphere through dry porous surface soil (Fig. 5). Complete oxidation of $Fe^{2+}_{aq}$ would produce $\delta^{56}$Fe values equal to those of the initial $Fe^{2+}_{aq}$, but these are expected to be less than or equal to zero, as noted above. The positive $\delta^{56}$Fe values for the Fe-enriched sections instead suggest that only partial oxidation occurred. The net $Fe^{3+}_{oxide}$–$Fe^{2+}_{aq}$ fractionation at room temperature generally lies between +1.0 and +2.0‰, occasionally as high as +3.0‰, as observed in experiment or the field [39,43,44], reflecting a combined $Fe^{3+}_{aq}$–$Fe^{2+}_{aq}$ fractionation and $Fe^{3+}_{oxide}$–$Fe^{3+}_{aq}$ fractionation, where the later often reflects kinetic effects [30]. Assuming a Rayleigh model and an initial $\delta^{56}$Fe value for $Fe^{2+}_{aq}$ that was zero, the average $\delta^{56}$Fe value for the Fe-enriched section ($\delta^{56}$Fe ~+0.3‰) can be produced by ~90% oxidation and precipitation using a $Fe^{3+}_{oxide}$–$Fe^{2+}_{aq}$ fractionation factor of +1.5‰. If the initial $\delta^{56}$Fe value of $Fe^{2+}_{aq}$ was −1.0‰, the average $\delta^{56}$Fe value for the Fe-enriched section may be produced by ~20% oxidation and precipitation. In all cases, such a model requires the existence of a large reservoir of low-$\delta^{56}$Fe $Fe^{2+}_{aq}$ outside of the exposed paleosol section to balance the positive $\delta^{56}$Fe values for the samples that were analyzed.

The consistently positive $\delta^{56}$Fe values for the Hekpoort paleosol contrasts with the commonly negative $\delta^{56}$Fe values that are found in acid-extractable Fe in modern soils (Fig. 4). In modern soils, $Fe^{3+}$ that is bound to organics or occurs in $Fe^{3+}$ oxides appear to have negative $\delta^{56}$Fe values [34], reflecting the isotopic effects of organic ligands [32,33] or complete oxidation of low-$\delta^{56}$Fe $Fe^{2+}_{aq}$ produced by $Fe^{3+}$-reducing bacteria

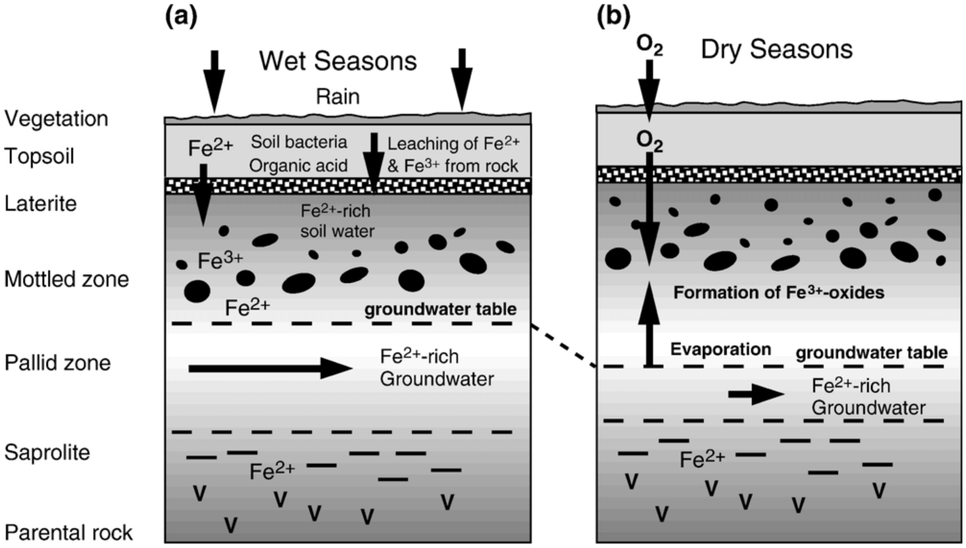

Fig. 5. Schematic model showing process of laterite formation in multiple cycles of (a) wet seasons and (b) dry seasons, adapted from Beukes et al. [12]. In wet seasons, removal of low-$\delta^{56}$Fe iron through mobilization by organic acids and/or $Fe^{3+}$-reducing bacteria would produce a residue that had low Fe contents but high $\delta^{56}$Fe values, producing the "Fe-depleted group" in Fig. 4. During the dry seasons, interaction between $Fe^{2+}$-rich groundwaters and infiltrating atmospheric $O_2$ would produce high-$\delta^{56}$Fe, Fe-rich oxides if partial oxidation of $Fe^{2+}_{aq}$ occurred, producing the "Fe-enriched group" in Fig. 4.

[13]. We interpret the contrast with modern soil profiles to reflect differing extents of fluid–rock interaction and net Fe transport. Mobilization of low-$\delta^{56}$Fe iron in modern soil profiles seem likely to be limited due to *in situ* oxidation, which would mitigate overall loss of low-$\delta^{56}$Fe components from the system. In addition, paleosols such as the Hekpoort section likely reflect a longer timescale of Fe cycling than revealed by studies of modern soil profiles.

### 5.3. Constraints on Atmospheric $O_2$?

Calculation of ancient $pO_2$ levels from paleosol sections requires estimates of $O_2$ transport processes from the surface and the molar balance of $Fe^{2+}$ and $Fe^{3+}$ [1,2]. The open-system behavior for Fe that is demonstrated by the isotopic data indicates that additional $O_2$ was required to oxidize $Fe^{2+}$ beyond that calculated by [1], who assumed closed-system oxidation of silicate $Fe^{2+}$ from the parental basalt. Yang and Holland [1] used an average (initial) rock concentration of 1.05 mol/kg FeO as the basis for their estimated $O_2$ loss during weathering of 0.06 mol $O_2$/kg rock. The total $O_2$ required to oxidize the parental basalt and the additional $Fe^{2+}$ that was transported into the paleosol section by aqueous fluids can be expressed as:

$$M_{O2}^{Tot} = 0.25 \cdot M_{Fe}^{Add} + M_{O2}^{Y\&H} \tag{1}$$

where $M_{O2}^{Y\&H}=0.06$ from Yang and Holland [1] and the 0.25 coefficient is based on the stoichiometry of oxidation of $Fe^{2+}$:

$$Fe_{aq}^{2+} + 5/2H_2O + 1/4O_2 \rightarrow Fe(OH)_3 + 2H^+ \tag{2}$$

or

$$FeO + 3/2H_2O + 1/4O_2 \rightarrow Fe(OH)_3 \tag{3}$$

Following the approach of Yang and Holland [1], the total $O_2$ required to oxidize the total Fe inventory is:

$$pO_2 = (M_{O2}^{Tot}/M_{CO2}) \cdot pCO_2 \tag{4}$$

where $M_{CO2}=4.18$ mol/kg rock and $pCO_2=2\times10^{-2}$ atm [13].

The minimum total $O_2$ required to form the Fe-enriched suite can be calculated using Eqs. (1) and (4) and the molar ratio of total $Fe^{3+}$ in the paleosol relative to the parental basalt, assuming 100% oxidation of $Fe_{aq}^{2+}$ occurred (Fig. 6). The molar ratio of total Fe to initial Fe ($M^{Fe}/M_i^{Fe}$) for the Fe-enriched suite ranges from 1.85 to 5.20. Over this range in $M^{Fe}/M_i^{Fe}$, the minimum total $O_2$ required to produce the highest Fe contents in the Fe-enriched suite varies from 1.6 to 19.4 times that calculated by Yang and Holland [1] relative to their $pO_2$ estimates of $9\times10^{-3}$ to $2.5\times10^{-4}$ atm, assuming 100% oxidation of $Fe_{aq}^{2+}$ (Fig. 6). This is equivalent to a $pO_2$ level as high as 0.07 relative to present atmosphere levels (PAL) (Fig. 6). Because such an estimate is a linear function of $pCO_2$ level (Eq. (4)), ranges for $pCO_2$ levels of 0.01–0.03 atm (*i.e.*, 30–100 PAL; [1]) or >0.03 atm (*i.e.*, >100 PAL; [45]) become equivalent to $pO_2$ levels of 0.035–0.105 PAL or >0.105 PAL. We note that these calculations are cast in terms of the assumptions made by Yang and Holland [1] so that the effect of external Fe may be highlighted, and are not intended to be a rigorous model of open-system behavior in the paleosol.

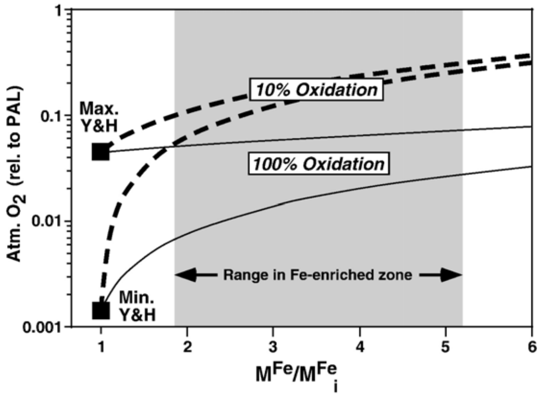

Fig. 6. Dependency of atmospheric $pO_2$ (expressed relative to Present Atmospheric Levels; PAL) on the molar ratio of $Fe^{3+}$ to initial Fe in the Hekpoort basalt, as calculated using Eqs. (1) and (4) in the text. The minimum and maximum estimates for $pO_2$ from Yang and Holland [1] are noted, where their calculations assume a closed system relative to Fe ($M^{Fe}/M_i^{Fe}=1$). Range in $M^{Fe}/M_i^{Fe}$ for the Fe-enriched suite shown by gray field. Solid curves indicate range in $pO_2$ levels calculated assuming 100% oxidation of external $Fe^{2+}{}_{aq}$ produced the Fe-enriched suites. Dashed curves indicate range of $pO_2$ levels calculated assuming that the Fe-enriched suite was produced by 10% oxidation of $Fe_{aq}^{2+}$, followed by complete oxidation outside the measured paleosol section.

The consistently positive $\delta^{56}$Fe values for the Fe-enriched suite provide strong evidence that the external $Fe_{aq}^{2+}$ that was added was only partially oxidized, raising the possibility that even larger quantities of $O_2$ may have been involved if oxidation occurred outside the measured section. As an illustration, if the Fe-enriched suite was produced by 10% oxidation of $Fe_{aq}^{2+}$, with the remaining $Fe_{aq}^{2+}$ oxidized outside the measured section, $pO_2$ levels could have been as high as $5–6\times10^{-2}$ atm, as calculated using Eqs. (1) and (4). This is equivalent to 0.27 to 0.31 PAL (Fig. 6). Although it is difficult to place upper bounds on $pO_2$ levels because of uncertainties in modeling the open-system behavior of the Hekpoort paleosol, these simple calculations illustrate the importance of external Fe sources in estimating $pO_2$ using the Yang and Holland [1] approach.

The most robust constraints on $pO_2$ levels can only be obtained on paleosol sections that remained closed with respect to Fe, which would be expected to have minimally variable Fe isotope compositions whose average $\delta^{56}$Fe value was near zero. Iron isotopes can provide strong constraints on which paleosols meet this criteria.

## 6. Conclusions

Mobility of the redox-sensitive element Fe in Precambrian paleosol profiles has been a major component to discussions on the oxygen contents of the ancient atmosphere (*e.g.*, [2]). The homogenous Fe isotope composition of the igneous Fe inventory in the Earth [46,47], as well as most bulk sedimentary rocks that are low in $C_{org}$ or $C_{carb}$ contents of Archean to modern age [27,28], provide a powerful baseline composition for evaluating open- or closed-system behavior of Fe in Precambrian paleosols.

An oxidant was present at the time of formation of the Hekpoort paleosol as indicated by enrichment of $Fe^{3+}$-oxides and the commonly positive $\delta^{56}$Fe values measured in this study, given the positive $Fe^{3+}$-$Fe^{2+}$ isotope fractionation factors for Fe-bearing solutions and minerals that are common in nature (*e.g.*, [13]). At the same time, however, positive $\delta^{56}$Fe values for oxides indicate an open system with respect to Fe, hindering estimates of $pO_2$ levels based on the assumption that only *in situ* oxidation of the parental basalt occurred [1]. Transport of $Fe^{2+}$-rich groundwater through soil, followed by oxidative precipitation of Fe, seems the most likely explanation for producing the $Fe^{3+}$-enriched sections of the paleosol that also have high-$\delta^{56}$Fe values. We therefore interpret the lateritic paleoweathering profile in Gaborone, Botswana, to reflect oxidative weathering of the parental basalt under an atmosphere that had significantly higher $O_2$ levels than previously estimated, where organic acids and/or bacterial $Fe^{3+}$ reduction produced low-$\delta^{56}$Fe components such as $Fe^{2+}_{aq}$, consistent with evidence for a terrestrial biosphere [48–51]. The evidence for significant Fe mobility, including addition of external sources of Fe, indicates that previous estimates for $pO_2$ of $2.5\times10^{-4}$ to $9\times10^{-3}$ atm [1] are too low by at least an order of magnitude. The results of the current study demonstrate that only paleosols that have restricted Fe isotope variations, whose average $\delta^{56}$Fe value lies near the crustal average ($\delta^{56}Fe=0$), should be considered when estimating past $pO_2$ levels from ancient soil or weathering profiles.

## Acknowledgments

This study was financially supported by a NASA-Ames Joint Research Initiative to CMJ, BLB, and KEY, the NASA Astrobiology Institute (NCC2-1057 and NNA04CC06A), the NASA Exobiology Program (NAG5-9089), the NSF Geochemistry Program (EAR-9706279 and EAR-0229556) to HO, the Japanese Ministry of Education, Culture, Sports, Science and Technology (MEXT), and the Japan Society for the Promotion of Science (JSPS) to KEY. A major part of this study was performed during KEY's postdoctoral stay at the University of Wisconsin–Madison, and the manuscript was completed during his tenure at IFREE–JAMSTEC, Japan. We thank two anonymous reviewers for their constructive comments that helped to polish the earlier manuscript, and Rick Carlson for editorial handling.

## References

[1] W. Yang, H.D. Holland, The Hekpoort paleosol profile in Strata 1 at Gaborone, Botswana: soil formation during the great oxidation event, Am. J. Sci. 303 (2003) 187–220.

[2] R. Rye, H.D. Holland, Paleosols and the evolution of atmospheric oxygen: a critical review, Am. J. Sci. 298 (1998) 621–672.

[3] H.D. Holland, N.J. Beukes, A Paleoweathering Profile from Griqualand West, South-Africa — evidence for a dramatic rise in atmospheric oxygen between 2.2 and 1.9 Bybp, Am. J. Sci. 290A (1990) 1–34.

[4] H.D. Holland, The Chemical Evolution of the Atmosphere and Oceans, Princeton University Press, Princeton, 1984 582 pp.

[5] A. Button, Early Proterozoic weathering profile on the 2200 m.y. old Hekpoort Basalt, Pretoria Group, South Africa: preliminary results, Economic Geology Research Unit Circular, University of Witwatersrand, 1979, p. 19.

[6] A. Bekker, H.D. Holland, P.L. Wang, D. Rumble, H.J. Stein, J.L. Hannah, L.L. Coetzee, N.J. Beukes, Dating the rise of atmospheric oxygen, Nature 427 (2004) 117–120.

[7] H.D. Holland, Early Proterozoic atmospheric change, in: S. Bengston (Ed.), Early Life on Earth, Nobel Symposium, vol. 84, Columbia University Press, New York, 1994, pp. 237–244.

[8] H.D. Holland, Volcanic gases, black smokers, and the great oxidation event, Geochim. Cosmochim. Acta 66 (2002) 3811–3826.

[9] H. Ohmoto, When did the Earth's atmosphere become toxic? Geochem. News 93(1997) 12–13; 26–27.

[10] G.N. Phillips, J.D.M. Law, R.E. Myers, Is the redox state of the Archean atmosphere constrained? Soc. Econ. Geol. Newsl. 47 (2001).

[11] R. Rye, H.D. Holland, Geology and geochemistry of paleosols developed on the Hekpoort basalt, Pretoria Group, South Africa, Am. J. Sci. 300 (2000) 85–141.

[12] N.J. Beukes, H. Dorland, J. Gutzmer, M. Nedachi, H. Ohmoto, Tropical laterites, life on land, and the history of atmospheric oxygen in the Paleoproterozoic, Geology 30 (2002) 491–494.

[13] C.M. Johnson, B.L. Beard, Fe isotopes: an emerging technique in understanding modern and ancient biogeochemical cycles, GSA Today 16 (2006) 4–10.

[14] A. Button, A Regional Study of the Stratigraphy and Development of the Transvaal Basin in Eastern and Northeastern Transvaal, University of Witwatersrand, 1973.

[15] H. Wiggering, N.J. Beukes, Petrography and geochemistry of a 2000–2200 Ma-old hematite paleo-alteration profile on Ongeluk

basalt of the Transvaal Supergroup, Griqualand West, South Africa, Precambrian Res. 46 (1990) 241–258.
[16] H. Dorland, Paleoproterozoic Laterite, Red Beds, and Ironstone of the Pretoria Group with Reference to the History of Atmospheric Oxygen, Rand Afrikans University, 1999.
[17] D.A. Evans, N.J. Beukes, J.L. Kirschvink, Low-latitude glaciation in the Palaeoproterozoic era, Nature 386 (1997) 262–266.
[18] D.A.D. Evans, N.J. Beukes, J.L. Kirschvink, Paleomagnetism of a lateritic paleoweathering horizon and overlying Paleoproterozoic red beds from South Africa: Implications for the Kaapvaal apparent polar wander path and a confirmation of atmospheric oxygen enrichment, J. Geophys. Res., Solid Earth 107 (2002), doi:10.1029/2001JB000432.
[19] D.H. Cornell, S.S. Schutte, B.L. Eglington, The Ongeluk basaltic andesite formation in Griqualand West, South Africa: Submarine alteration in a 2222 Ma Proterozoic sea, Precambrian Res. 79 (1996) 101–123.
[20] F. Walraven, Geochemistry of the Rooiberg Group, Transvaal Supergroup, South Africa, Economic Geology Research Unit Information Circular, vol. 316, University of Witwatersrand, 1997, p. 21.
[21] G.J.J. Aleva, Laterites: Concepts, geology, morphology, and chemistry, International Soil Reference and Information Centre, Wageningen, 1994, p. 169.
[22] L.C. Stookey, Ferrozine — a new spectrophotometric reagent from iron, Anal. Chem. 42 (1970) 779–781.
[23] F. Albarede, B. Beard, Analytical methods for non-traditional isotopes. Geochemistry of Non-Traditional Stable Isotopes, Rev. Mineral. Geochem. 55 (2004) 113–152.
[24] B.L. Beard, C.M. Johnson, J.L. Skulan, K.H. Nealson, L. Cox, H. Sun, Application of Fe isotopes to tracing the geochemical and biological cycling of Fe, Chem. Geol. 195 (2003) 87–117.
[25] B.L. Beard, C.M. Johnson, Inter-mineral Fe isotope variations in mantle-derived rocks and implications for the Fe geochemical cycle, Geochim. Cosmochim. Acta 68 (2004) 4727–4743.
[26] F. Poitrasson, R. Freydier, Heavy iron isotope composition of granites determined by high resolution MC–ICP–MS, Chem. Geol. 222 (2005) 132–147.
[27] B.L. Beard, C.M. Johnson, K.L. Von Damm, R.L. Poulson, Iron isotope constraints on Fe cycling and mass balance in oxygenated Earth oceans, Geology 31 (2003) 629–632.
[28] K.E. Yamaguchi, C.M. Johnson, B.L. Beard, H. Ohmoto, Biogeochemical cycling of iron in the Archean–Paleoproterozoic Earth: constraints from iron isotope variations in sedimentary rocks from the Kaapvaal and Pilbara Cratons, Chem. Geol. 218 (2005) 135–169.
[29] K.E. Yamaguchi, H. Ohmoto, Geochemical and isotopic constraints on the origin of Paleoproterozoic red shales of the Gamagara/Mapedi Formation, Postmasburg Group, South Africa, S. Afr. J. Geol. 109 (2006) 123–138.
[30] B.L. Beard, C.M. Johnson, Fe isotope variations in the modern and ancient earth and other planetary bodies. Geochemistry of Non-Traditional Stable Isotopes, Rev. Mineral. Geochem. 55 (2004) 319–357.
[31] M.S. Fantle, D.J. DePaolo, Iron isotopic fractionation during continental weathering, Earth Planet. Sci. Lett. 228 (2004).
[32] S.L. Brantley, L. Liermann, T.D. Bullen, Fractionation of Fe isotopes by soil microbes and organic acids, Geology 29 (2001) 535–538.
[33] S.L. Brantley, L.J. Liermann, R.L. Guynn, A. Anbar, G.A. Icopini, J. Barling, Fe isotopic fractionation during mineral dissolution with and without bacteria, Geochim. Cosmochim. Acta 68 (2004) 3189–3204.
[34] S. Emmanuel, Y. Erel, A. Matthews, N. Teutsch, A preliminary mixing model for Fe isotopes in soils, Chem. Geol. 222 (2005) 23–34.
[35] M.A. Chan, C.M. Johnson, B.L. Beard, J.R. Bowman, W.T. Parry, Iron isotopes constrain the pathways and formation mechanisms of terrestrial oxide concretions: a tool for tracing iron cycling on Mars? Geosphere 2 (2006) 324–332.
[36] S. Severmann, C.M. Johnson, B.L. Beard, J. McManus, The effect of early diagenesis on the Fe isotope compositions of porewaters and authigenic minerals in continental margin sediments, Geochim. Cosmochim. Acta 70 (2006) 2006–2022.
[37] M. Staubwasser, F. von Blanckenburg, R. Schoenberg, Iron isotopes in the early marine diagenetic iron cycle, Geology 34 (2006) 629–632.
[38] B. Mamet, A. Preat, Iron-bacterial mediation in Phanerozoic red limestones: state of the art, Sediment. Geol. 185 (2006) 147–157.
[39] T.D. Bullen, A.F. White, C.W. Childs, D.V. Vivit, M.S. Schulz, Demonstration of significant abiotic iron isotope fractionation in nature, Geology 29 (2001) 699–702.
[40] J.G. Wiederhold, S.M. Kraemer, N. Teutsch, P.M. Borer, A.N. Halliday, R. Kretzschmar, Iron isotope fractionation during proton-promoted, ligand-controlled, and reductive dissolution of goethite, Environ. Sci. Technol. 40 (2006) 3787–3793.
[41] H.A. Crosby, C.M. Johnson, E.E. Roden, B.L. Beard, Coupled Fe(II)–Fe(III) electron and atom exchange as a mechanism for Fe isotope fractionation during dissimilatory iron oxide reduction, Environ. Sci. Technol. 39 (2005) 6698–6704.
[42] C.M. Johnson, E.E. Roden, S.A. Welch, B.L. Beard, Experimental constraints on Fe isotope fractionation during magnetite and Fe carbonate formation coupled to dissimilatory hydrous ferric oxide reduction, Geochim. Cosmochim. Acta 69 (2005) 963–993.
[43] L.R. Croal, C.M. Johnson, B.L. Beard, D.K. Newman, Iron isotope fractionation by Fe(II)-oxidizing photoautotrophic bacteria, Geochim. Cosmochim. Acta 68 (2004) 1227–1242.
[44] N. Balci, T.D. Bullen, K. Witte-Lien, W.C. Shanks, M. Motelica, K.W. Mandernack, Iron isotope fractionation during microbially stimulated Fe(II) oxidation and Fe(III) precipitation, Geochim. Cosmochim. Acta 70 (2006) 622–639.
[45] H. Ohmoto, Y. Watanabe, K. Kumazawa, Evidence from massive siderite beds for a CO2-rich atmosphere before, 1.8 billion years ago, Nature 429 (2004) 395–399.
[46] B.L. Beard, C.M. Johnson, Comment on “Heavy iron isotope composition of granites determined by high resolution MC–ICP–MS”, by F. Poltrasson and R. Freydier [Chem. Geol. 222 132–147], Chem. Geol. 235(2006) 201–204.
[47] F. Poitrasson, On the iron isotope homogeneity level of the continental crust, Chem. Geol. 235 (2006) 195–200.
[48] H. Ohmoto, Evidence in pre-2.2 Ga paleosols for the early evolution of atmospheric oxygen and terrestrial biota, Geology 24 (1996) 1135–1138.
[49] J. Gutzmer, N.J. Beukes, Earliest laterites and possible evidence for terrestrial vegetation in the Early Proterozoic, Geology 26 (1998) 263–266.
[50] Y. Watanabe, J.E.J. Martini, H. Ohmoto, Geochemical evidence for terrestrial ecosystems 2.6 billion years ago, Nature 408 (2000) 574–578.
[51] Y. Watanabe, B.W. Stewart, H. Ohmoto, Organic-and carbonate-rich soil formation similar to 2.6 billion years ago at Schagen, East Transvaal district, South Africa, Geochim. Cosmochim. Acta 68 (2004) 2129–2151.